Applied Mechanics and Materials
ISSN: 1662-7482, Vol. 307, pp 352-357
doi:10.4028/www.scientific.net/AMM.307.352
Online: 2013-02-13

Calorimetric Analysis of Precipitation in Undercooled Ni-Si Alloy

Kai Fan[1, 3a], Feng Liu[2,b], Baoquan Fu[1,2,c], Wenzhong Luo[1, d] and Yaohe Zhou[2,e]

[1] Shaanxi Province Engineering Laboratory for Aerial Material, Western Superconducting Technologies Co., Ltd, Xi'an 710018, China

[2]Key Laboratory of Solidification Processing, Northwestern Polytechnical University, Xi'an, Shaanxi 710072, P.R.China

[3]National Engineering Laboratory for Superconducting Material, Western Superconducting Technologies Co., Ltd, Xi'an 710018, China

[a]fankai@mail.nwpu.edu.cn, [b]liufeng@nwpu.edu.cn, [c]bqfu@c-nin.com, [d]luowz808@yahoo.com.cn, [e]yhzhou@nwpu.edu.cn

Keywords: undercooling, precipitation, soft impingement, Ni-Si alloy.

Abstract. In order to study the precipitaion of Ni_3Si particle in undercooled Ni-Si alloy, calorimetric analyses were carried out using non-isothermal measurements by DSC. The scanning electron microscopy (SEM) and the transmission electron microscopy (TEM) measurements were used to describe qualitatively and quantitatively the precipitate microstructures. The non-isothermal DSC thermograms exhibited one reaction peaks and it indicated that the precipitation process is an exothermic reaction. The evolution for the precipitate was obtained in the as-solidified Ni-Si alloy subjected to ΔT=195K, meanwhile, the precipitate size was found increased with decreased heating rate in the TEM images. The largest precipitate size was about 120nm, and the precipitates still kept spherical shape. Model prediction for the precipitation of Ni_3Si particle has been performed. Good agreement with experimental data has been achieved.

Introduction

As is well known, non-equilibrium solidification has been successfully applied to produce metastable materials (e.g. supersaturated solid solutions and amorphous alloys) from liquid state [1]. The initial condition and the characteristics of such metastable solids are different from that by conventional solidification, i.e. the solid solubility, the structural defect and the solute segregation are all strengthened upon non-equilibrium solidification [2], which further influence the nucleation and growth of precipitates in the subsequent solid–state transformation.

As a typical nucleation/growth controlled process, the precipitation is well known as the formation of new-phase particles from supersaturated solid solution [3-6]. Deep understanding of the nucleation and growth kinetics of precipitates can improve the mechanical properties and optimize the process control, and therefore acquire suitable capabilities of products [3]. So far, our theoretical works about the precipitation kinetics were mainly focused on the soft impingement model [7-10]. In view of the previous works, it must be noted that, any precipitation from the supersaturated solid solution is connected with the solute distribution, which inevitably refers to the initial condition of the matrix phase[11-16]. That is to say, the initial condition of the matrix phase directly determines the precipitation of the second phase.

Due to the preparation of matrix phase subjected to different undercoolings, ΔTs, and the subsequent investigation on precipitation in the matrix phase open a window for studying the effect of non-equilibrium solidification on subsequent precipitation kinetics, an our recent work was focused on the microstructure evolution of Ni-Si hypoeutectic alloy melt and the precipitation of Ni_3Si particle in the as-solidified alloy upon isothermal annealing, therefore, the effect of non-equilibrium solidification on solid-state precipitation kinetics of Ni_3Si particle was declared, by combination of non-equilibrium dendrite growth theory with analytical soft impingement model[9]. So in this work, we aimed to describe the precipitation of Ni_3Si particle in the as-solidified alloy upon non-isothermal annealing, which further declared the effect of non-equilibrium solidification on solid-state precipitation kinetics of Ni_3Si particle.

Experimental procedure

The DSC was used to follow the precipitation sequence that takes place in an undercooled Ni-18at.%Si alloy during continuous heating at constantheating rates. Disc shaped DSC samples of 4.5 mm dia. And ~1.0 mm thickness of average mass ~35 mg were machined from the as-solidified Ni-Si hypoeutectic alloy melt subjected to ΔT ~195K. An annealed pure aluminium disc of similar shape and mass was used as a reference. Non-isothermal scanning techniques were performed for the specimens using a DSC thermal analyser (DSC STA449C, Netzsch, German) at heating rates of 10, 15, 20 and 80 K/min. DSC scans were started at room temperature and completed at 1273K under a purified argon gas atmosphere flowing at a rate of 80 ml min^{-1}. The output was in mW and the net heat flow to the reference material (pure Al) relative to the sample was recorded as a function of temperature. The peak temperatures of the reaction processes were determined with an accuracy of $\pm$0.1 K using the microprocessor of the thermal analyser.

After the DSC tests, specimens for TEM observations were prepared by 656 dimple grinder and the conventional twin-jet technique (GATAN, USA). The evolution of precipitate was observed using SUPRA-55 field emission scanning electron microscope (FESEM) (IEISS, Germany) and TECNAI F30 G^2 transmission electronic microscopy (TEM) (FEI, USA). Specimens for scanning electron microscope were mechanically polished and etched by a 1:2:3 (vol.%) H_3NO_3:HF:$C_3H_5(OH)_3$ solution.

Theory background

Following Ref.[10], a model to treat soft impingement (overlapping diffusion fields) in non-isothermal solid-state precipitation can be classified as the first stage (FS) and the second stage (SS). In FS, the size of the second-phase particle r^I is less than the critical size r_z, giving non-overlapping diffusion fields. The transformed fraction f during the parabolic growth stage is given as [10],

$$f=\left(\frac{r^I}{r_f}\right)^d=\left(\left\{\frac{\lambda_d^2 R}{\Phi Q_D}\left[T^2 D(T)-T_0^2 D(T_0)\right]\right\}^{1/2}\Big/ r_f\right)^d \tag{1}$$

where, λ_d, as function of the pertinent concentration, is defined as the growth coefficient. $D(T)$ is the temperature-dependent diffusion coefficient, it follows an Arrhenius relationship, i.e., $D(T)$= $D_0\exp[-Q_D/(RT)]$, D_0 is the pre-exponential factor for diffusion. Both D_0 and Q_D are assumed to hold constant during the non-isothermal transformation. $r_f = L\xi^{1/d}$ and ξ =[($(C^m$- C^α)/(C^β-C^α)]}.

If r^I=r_z, the diffusion fields start to overlap [10], the critical size r_z has be given as

$$r_z=\left(\frac{C^m-C^\alpha}{2C^\beta-C^\alpha-C^m}\right)^{1/d}L \tag{2}$$

where, $2L$ is defined as a distance between two particles, inferring that the maximum size (in r direction) for the matrix should be L. C^m is the saturated composition in a single-phase alloy before transformation, and C^β and C^α are the equilibrium solute concentration of the product phase β and the parent phase α after the transformation.

Once r^I≥r_z, SS is reached, the size of the second-phase particle becomes larger than r_z, giving overlapping diffusion fields and in turn retarding the transformation rate. According to Ref.[10], the evolution of transformed fraction f with T during soft impingement have be given as,

$$f=\left(\frac{r^I}{r_f}\right)^d=1-\frac{C}{2}\exp\left\{-\frac{kR}{\Phi^2 Q_D}\left[T^2 D(T)-T_1^2 D(T_1)\right]\right\}. \tag{3}$$

where k=C_1k_1 with C_1 as a correction factor. C and k have been derived as $2[1-(r_z/r_f)^d]$ and $\lambda_d^2\Phi(d/2)(r_z/r_f)^d[1-(r_z/r_f)^d]^{-1}/r_z^2$, respectively.

If $T=T_f$ and $r=r_f$, the solute content in the parent phase is uniform and equal to C^{α}. A physical correlation among T_0, T_f, r_z and Φ is not clear, but from Eq.(1), a critical cooling/heating rate Φ_z can be given to determine the occurrence of soft impingement. Substitution of $r^{\mathrm{I}}=r_z$ into Eq.(2) leads to,

$$\Phi_z = \frac{\lambda_d^2 R}{r_z^2 Q_D}\left[T_f^2 D(T_f) - T_0^2 D(T_0)\right]. \tag{4}$$

Corresponding to a specific stage, T_f and r_z, Eq.(4) implies that if $|\Phi|<|\Phi_z|$, the diffusion fields overlap; therefore the effect of soft impingement must be taken into account and vice versa. A rearrangement of Eqs.(1) and (3) gives,

$$\begin{aligned} f_m = \left(\frac{r_f}{L}\right)^d &= \Xi(T)\left\{\left[\frac{\lambda_d^2 R}{Q_D}\left|T_f^2 D(T_f) - T_0^2 D(T_0)\right|\right]^{½} \Big/ L\right\}^d |\Phi|^{-\frac{d}{2}} \\ &+ (1-\Xi(T))\left\{1 - \frac{C}{2}\exp\left[-\left(A_1|\Phi|^{-2} + A_2|\Phi|^{-1}\right)\right]\right\}\xi \end{aligned} \tag{5}$$

where f_m is the expected transformed fraction corresponding to T_f, $A_1=\lambda_d^2 R|k||T_f^2 D(T_f))-T_0^2 D(T_0)|/Q_D$, $A_2=|k|r_z^2$. Obviously, for a given T_f, the value of f_m is decreased with increasing $|\Phi|$; $\Xi(t)=0$ if $|\Phi|<|\Phi_z|$ and $\Xi(t)=1$ if $|\Phi|\geq|\Phi_z|$ (*c.f.* Eq.(14)). So, Eq.(5) can be adapted to predict the cooling/heating rate necessary to control the soft impingement during the transformation.

Results and Discussion

Typical non-isothermal thermograms performed at heating rates of 10K/min are shown in Fig. 1. It shows one reaction phase transformation which is exothermic reaction labelled run 2 in Fig.1. The scanning rate test was carried out two cycles (i.e., run1 and run2 in Fig.1). The first cycle corresponded to heating empty corundum crucible presents no exothermic reaction (run 1), subsequently, the second cycle corresponded to heating corundum crucible with the as-solidified Ni-Si alloy subjected to ΔT=195K specimen placed in presents an exothermic reaction (run 2). It is believed that the exothermic peak is related to the precipitation of the Ni_3Si phase (Fig.2).

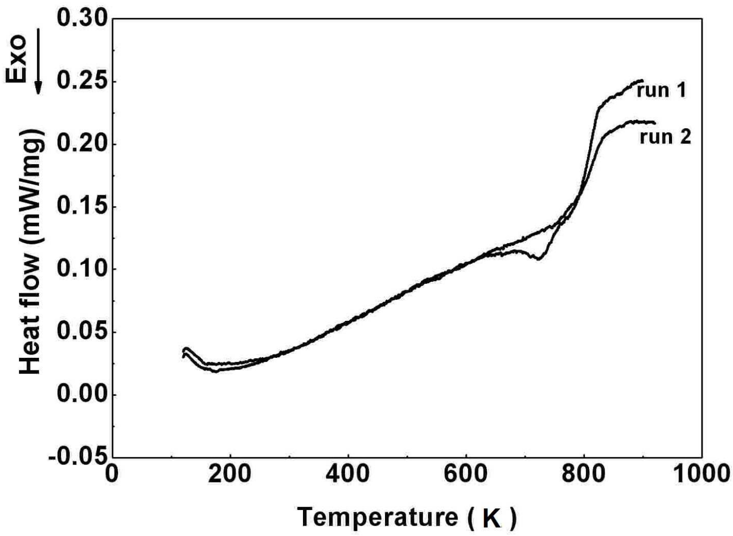

Fig.1 DSC curves for the precipitation of Ni_3Si particle in the undercooled alloy of 195K at a heating rate of 10K/min

The typical microstructure evolution studied under SEM after the DSC measurements is shown in Fig. 2. It shows that the precipitate size was found increased with decreased heating rate in the SEM images. The precipitate size corresponded to heating rate of 30K/min is very small, it can be hardly observed through SEM (Fig.2 (a)). The precipitate size corresponded to heating rate achieved 15K/min is large enough to be observed through SEM (Fig.2 (c)).

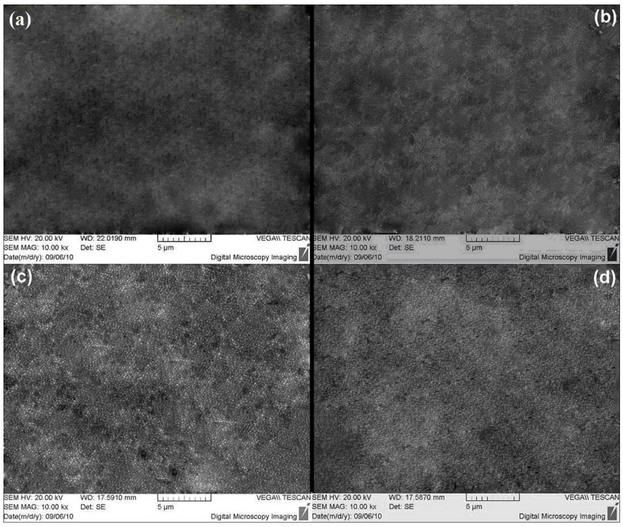

Fig.2 Scanning electron photographs of the Ni_3Si precipitates in the undercooled alloy of 195K under different heating rates: (a)30K/min, (b)20K/min, (c)15K/min, (d)10K/min

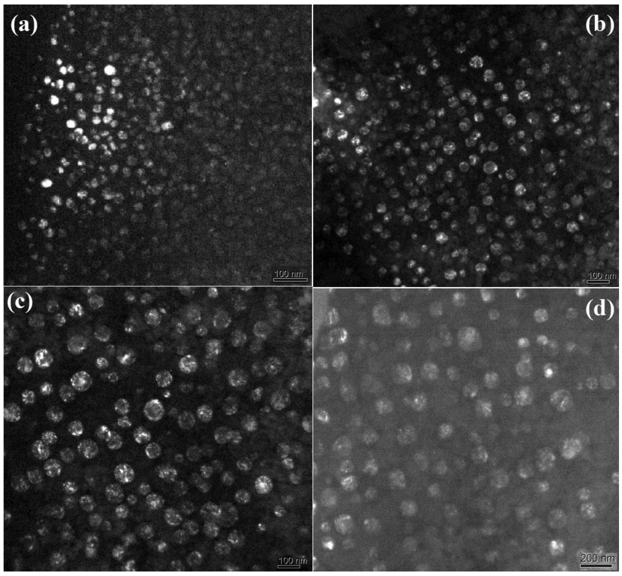

Fig. 3 Dark-field TEM photographs of the Ni_3Si precipitates in the undercooled alloy of 195K under different heating rates: (a)30K/min, (b)20K/min, (c)15K/min, (d)10K/min

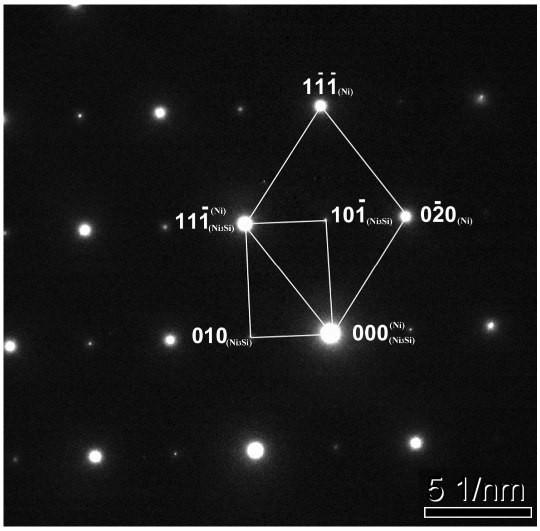

Fig. 4 Diffraction pattern showing reflections from both matrix and precipitate, (101)-oriented electron diffraction patterns from the Ni_3Si particles.

After the DSC measurements, dark-field TEM photographs of the Ni_3Si precipitates in the undercooled alloy of 195K under different heating rates are shown in Fig.3. The precipitate size is increased with decreased heating rate. The precipitates with the size of ~23nm are perfectly spherical at the heat rate of 30K/min (Fig.3a), and even when the heating rate decreases to 15K/min, the precipitates still keep spherical shape (Fig.3c). Further decreases the heating rate to 10K/min, the Ni_3Si particles with the size of ~120nm become slightly cubical (Fig.2d).

The corresponding electron diffraction pattern is shown in Fig.4, where both the Ni_3Si phase and the α-Ni matrix are demonstrated as f.c.c. lattice, and the Ni_3Si phase has the same Bravais lattice and almost the same lattice parameter as the α-Ni matrix (i.e. 0.3509nm for Ni_3Si phase and 0.3526nm for α-Ni matrix).

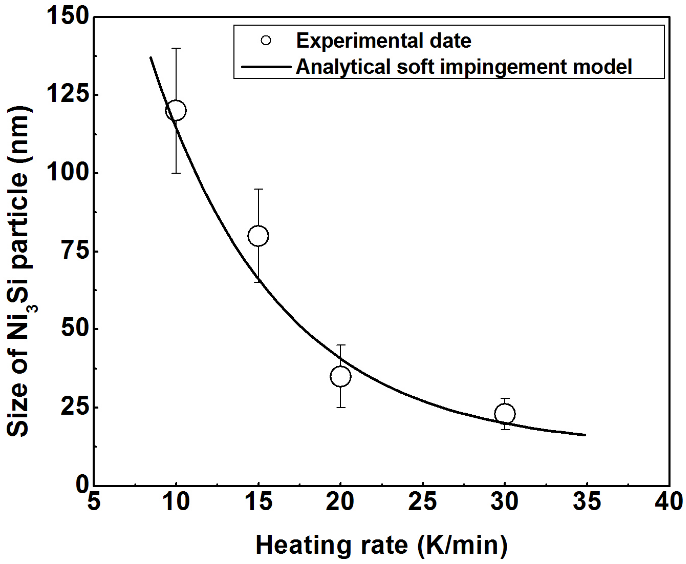

Fig.5 Evolution of the size of Ni_3Si particles at room temperature with different heating rates.

By means of analyzer (Image-Pro Plus 6.0), the final size of the precipitate of Ni_3Si r_f can be measured precisely from Fig. 3 (as shown in Fig.5). The Ni_3Si phase nucleates directly from the supersaturated solid solution, this precipitation mechanism is referred to as "continuous precipitation", and the Ni_3Si phase is in a spherical shape, so the 3-D model is just applicable (Eq(5)). Table 1 shows all the parameters used for 3-D modeling precipitation in undercooled Ni-Si alloy of 195K. The analytical soft impingement model is used to predict the evolution of the size of Ni_3Si particles, and it is good agreement with the experimental date (Fig.5).

Table 1. Parameters used for the current model prediction for σ-phase precipitation in a 2205 duplex stainless steel upon continuous cooling.

Parameter	Dimension	Value
The diffusion coefficient of Si in α(Ni) matrix D	m^2s^{-1}	4.28×10^{-15}[17]
The final size of the precipitates r_f	nm	300
The growth coefficient λ_3	/	-23.58
The nucleation density of Ni_3Si precipitate N^*	m^{-3}	1.38×10^{19}
The equilibrium concentration of Si in precipitates C^β	at.%	22.53[17]
The equilibrium concentration of Si in α(Ni) matrix C^α	at.%	9.92[17]
The concentration of Si in the matrix before transformation C^m	at.%	15.5[17]

Conclusions

Calorimetric analyses were carried out using non-isothermal measurements by DSC to study the precipitaion of Ni_3Si particle in undercooled Ni-Si alloy of 195K. The non-isothermal DSC thermograms exhibited one reaction peaks and it indicated that the precipitation process is an exothermic reaction. Tthe precipitate size was found increased with decreased heating rate in the TEM images. The largest precipitate size was about 120nm, and the shape of the precipitates becomes slightly cubical. Model prediction for the precipitation of Ni_3Si particle has been performed. Good agreement with experimental data has been achieved.

References

[1] Q.C. Li, C.S. Cui and D.M. Xu: J. Mater. Sci. Technol. Vol.14 (1998) p.49.

[2] D.M. Herlach: Mater. Sci. Eng. R Vol.12 (1994) p.177.

[3] J.W. Christian, The theory of transformation in metals and alloys, Pergamon Press,Oxford, (2002).

[4] F. Liu, F. Sommer, C. Bos and E.J. Mittemeijer: Int. Mater. Rev. Vol.52 (2007) p.193.

[5] Y.C. Guan and W. Zhou: Mater. Lett. Vol.62 (2008) p.4494.

[6] A. Gaber, K. Matsuda, A. M. Ali, Y. Zou and S. Ikeno: Mater. Sci. Technol. Vol.20 (2004) p.1627

[7] K. Fan, F. Liu, X.N. Liu, Y.X. Zhang, G.C. Yang and Y.H. Zhou: Acta Mater. Vol.56 (2008) p.4309.

[8] K. Fan, F. Liu, S.J. Song, G.C. Yang and Y.H. Zhou: J. Alloy Compds. Vol.491 (2010) p.L11.

[9] K. Fan, F. Liu, W. Yang, G.C. Yang and Y.H. Zhou: J. Mater. Res. Vol.24 (2009) p.3664.

[10] K. Fan, F. Liu, G.C. Yang and Y.H. Zhou: Mater. Sci. Eng. AVol.528 Vol.56 (2011) p.6844.

[11] F.S. Ham: J. Phys. Chem. Solids. Vol.6 (1958) p.335.

[12] J.H.Cho and A.J. Ardell: Acta Mater. Vol.16 (1998) p.5907

[13] P.K. Rastogi and A.J. Ardell: Acta Metall. Vol.24 (1990) p.321.

[14] C.W. Zheng, N.M. Xiao, L.H. Hao, D.Z. Li and Y.Y. Li: Acta Mater. Vol.57 (2009) p.2956.

[15] K.D. Li and E.Chang: Acta Mater. Vol.52 (2004) p.219.

[16] H. Sieurin and R. Sandström: Mater. Sci. Eng. A Vol.444 (2007) p.271.

[17] E.A. Brandes and G.B.Brook: Smithells metals reference book, London, Butterworths, (1992).